

Electronic Supplementary Information

Photosensitization mechanisms at the air-water interface of aqueous aerosols

Marilia T. C. Martins-Costa,[a] Josep M. Anglada,*[b] Joseph S. Francisco,[c] and Manuel F. Ruiz-López*[a].

[a] Laboratoire de Physique et Chimie Théoriques, UMR CNRS 7019, University of Lorraine, CNRS, BP 70239, 54506 Vandoeuvre-lès-Nancy, France

[b] Departament de Química Biològica IQAC-CSIC, c/ Jordi Girona 18, E-08034 Barcelona, Spain

[c] Department of Earth and Environmental Science and Department of Chemistry, University of Pennsylvania, Philadelphia, PA, USA 19104-631

Methodology

QM/MM Molecular Dynamics simulations

Molecular Dynamics (MD) simulations using the QM/MM approach have been described before.¹⁻⁵ The simulation box contains one IC molecule and 499 water molecules. IC is described quantum mechanically (QM system) at the B3LYP level⁶ with the 6-31G(d) basis set^{7, 8} (see Table S1 for the accuracy of this basis set). The water molecules are described classically through Molecular Mechanics (MM system) using a flexible version of the TIP3P force-field for water.^{9, 10} The box size is 24.71 x 24.71 x 24.71 Å in the bulk calculations, and we use periodic boundary conditions in the three directions. In the case of the interface, following usual procedures (see for instance Ref.¹¹), we use a rectangular box with the dimensions 24.71 x 24.71 x 130 Å, and we also use periodic boundary conditions. A water slab of (24.71 Å)³ is placed in the middle of the box. Therefore, the water slab is sandwiched between two sections of “vacuum” forming two interfaces. The Z-axis is assumed to be perpendicular to the interfaces. We assume a cutoff radius of 12.355 Å. Simulations have been done in the NVT ensemble at T=298K using the Nosé–Hoover thermostat.^{12, 13} The time step is 0.25 fs. The equilibration of the systems was carried out in the following way. We used a previously equilibrated water cubic box with its centre of mass placed at X=Y=Z=0 Å. In the case of the interface, we placed the IC molecule so that its centre of mass lies in the air layer (i. e., with X=Y=0, Z>>12.355 Å). The IC molecule is then slowly pushed towards the interface by carrying out QM/MM MD simulations with a harmonic bias potential of the form: $V = k (Z_{\text{CM}} - 13.0)^2$, where Z_{CM} is the Z-coordinate of a vector joining the centre of mass of the water molecules and the centre of mass of IC. We used $k = 10$ kcal/mol/Å². When Z_{CM} attained 13 Å, i. e. when IC nears the formal air-water interface plane, an equilibration trajectory was run for several tens of picoseconds to bring the system into thermal equilibrium (298K). During this equilibration trajectory, IC is restricted to move within the interface layer. After equilibration, the bias potential was removed. In the case of the bulk simulations, the procedure was similar except that the IC molecule was pushed directly into the water layer. Production trajectories were carried out for about 125 ps in the case of the singlet state IC(S₀). Due to a higher computational cost, the simulations for IC(T₁) were carried out for about 50 ps. The simulations are carried out using our home code¹⁴ that interfaces Gaussian 09¹⁵, and Tinker 4.2¹⁶ for the QM and MD calculations, respectively.

Snapshot set types

Snapshot set type 1: Snapshots were saved every 0.375 ps (i.e. 1500 steps) for further analysis along the IC(S₀) trajectory (total number of 330 snapshots from each trajectory, bulk or interface).

Snapshot set type 2: To analyse the oscillator strength fluctuations (Figure 7) and the spin-orbit couplings (SOC) (Table 3), 1000 snapshots were saved during 1 ps of the simulation (one snapshot per fs). For the SOC computations, we selected those snapshots for which there is at least one small singlet-triplet energy difference (below 10⁻³ au, total number of 137 snapshots in bulk water and 87 snapshots at the air-water interface).

MRCI computations, electronic spectra, spin-orbit coupling

The study of the excited states has been carried out using the MRCI (Multi Reference Configuration Interaction) method with the cc-pVTZ basis set,¹⁷ where the CI expansion has been done over B3LYP orbitals. In all cases, all valence electrons have been correlated but two different reference spaces have been chosen for generating the MRCI space. For the snapshot set type 1, it has been generated by single and double excitation from all 36 valence electrons in a set of 26 orbitals, whereas for the snapshot set type 2 it has been generated by single and double excitations from a CAS(8,6) space, which contain all configurations describing the electronic states of interest. In both cases, all valence electrons have been correlated, a cutoff threshold of 10⁻⁶ hartree has been used for determining the whole MRCI space, and the Davidson correction has been applied to account for higher excitations. The ORCA program package¹⁸ has been employed in these calculations. For the sake of comparison, in Table S1 we have collected the results obtained with the different MRCI approaches, at geometries optimized with the B3LYP functional using two different basis sets. The results correspond to gas phase calculations and the Table shows that all approaches lead to comparable results.

The excited states and UV-Vis spectra at the air-water interface and in bulk water have been obtained in the following way. For each saved snapshot in the QM/MM simulations (snapshot set type 1 and type 2), a combined MRCI/MM calculation is carried out to obtain the energy of the lowest singlet and triplet electronic states, as well as the oscillator strengths for the electronic transitions from the singlet ground state to the excited singlet states. The MRCI/MM calculation is done for a cluster containing IC plus all the water molecules present within a cutoff radius of 12 Å from the centre of mass of IC. IC is treated quantum mechanically (MRCI part), while water molecules are treated classically as point charges (MM part). The cc-pVTZ basis set¹⁷ is employed in these MRCI calculations.

The cross-section for each snapshot is obtained from the calculated oscillator strengths as indicated hereafter. The final spectra are obtained as an average of the calculated cross-sections for the selected snapshots (snapshot set type 1). Spin-orbit coupling (SOC) calculations for the set of selected snapshots (snapshot set type 2) have been carried out using the same MRCI/MM approach using the ORCA program package.¹⁸

Calculation of the cross-sections:

The dimensionless oscillator strength of an electronic transition is related to the integral of the absorption band according to the equation:¹⁹

$$f = \frac{4\epsilon_0 mc \ln 10}{N_a e^2} \int \epsilon(\nu) d\nu \quad (1)$$

where $\epsilon(\nu)$ is the molar absorption coefficient at wavenumber ν , m is the electron mass, e its charge, ϵ_0 the permittivity of vacuum, c the speed of light, and N_a Avogadro's constant. The relationship between the molecular absorption cross-section σ and the experimental value of ϵ is given by:¹⁹

$$\sigma = \frac{\epsilon \ln 10}{N_A} = 3.825 \times 10^{19} \epsilon \quad (2)$$

The units of ϵ are typically given in L·cm⁻¹·mol⁻¹, while units of σ are given in cm²·molecule⁻¹. One deduces:

$$f = 1.158 \times 10^{12} \int \sigma(\nu) d\nu \quad (3)$$

when σ is given in $\text{cm}^2 \cdot \text{molecule}^{-1}$ and ν in cm^{-1} . Now, if one assumes a Gaussian form for $\sigma(\nu)$ centred at ν_0 and having a full width half-maximum $\Delta\nu_{1/2}$, so that:

$$\sigma(\nu) = \sigma(\nu_0) e^{-\frac{2.773}{(\Delta\nu_{1/2})^2} (\nu - \nu_0)^2} \quad (4)$$

it follows from equation (3), after integrating the Gaussian from $-\infty$ to $+\infty$, that:²⁰

$$\sigma(\nu) = 0.811 \times 10^{-12} \frac{f}{\Delta\nu_{1/2}} e^{-2.773 \left(\frac{\nu - \nu_0}{\Delta\nu_{1/2}} \right)^2} \quad (5)$$

using $\text{cm}^2 \cdot \text{molecule}^{-1}$ for σ , and cm^{-1} for the wavenumbers.

The Gaussian width is a parameter that can be adjusted to fit the experimental cross-section using the calculated values of f . Previous studies at the same theoretical level have shown that this parameter is typically close to 0.6 eV,²¹⁻²⁴ and therefore in our computations we use this value ($\Delta\nu_{1/2} = 4839 \text{ cm}^{-1}$).

Table S1. Comparison of the gas phase relative energies and dipole moments of IC as a function of the computational level used to optimize the geometry. The MRCI computations have been done either at B3LYP/cc-pVTZ and at B3LYP/6-31G(d) optimized geometries.^a

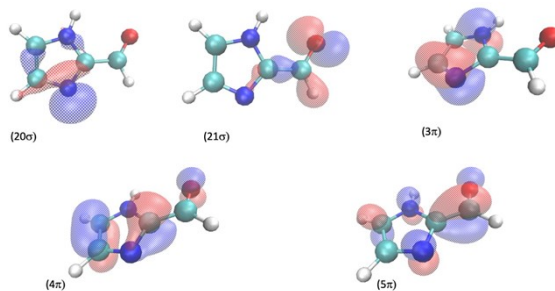
State	Main configuration	MRCI/cc-pVTZ // B3LYP/cc-pVTZ		MRCI/cc-pVTZ // B3LYP/6-31G(d)			
		ΔE (eV)	μ (D)	ΔE (eV)		μ (D)	
S₀	...20 σ^2 21 σ^2 3 π^2 4 π^2	0.00	2.99	0.00	<i>0.00</i>	2.95	2.98
S₁	...20 σ^2 3 π^2 4 π^2 21 σ 5 π	4.13	3.32	4.09	<i>4.11</i>	3.36	3.53
S₂	...20 σ^2 21 σ^2 3 π^2 4 π 5 π	4.80	7.95	4.73	<i>4.87</i>	7.91	7.74
T₁	...20 σ^2 21 σ^2 3 π^2 4 π 5 π	3.08	7.43	3.01	<i>3.07</i>	7.39	7.51
T₂	...20 σ^2 3 π^2 4 π^2 21 σ 5 π	3.51	3.36	3.47	<i>3.56</i>	3.40	3.64
T₃	...20 σ^2 21 σ^2 3 π 4 π^2 5 π	4.42	7.34	4.36	<i>4.55</i>	7.33	7.74

- a) The MRCI space has been generated from excitations of all 36 valence electrons as described above. Values in italics correspond to calculations where the MRCI space has been generated from a CAS(8,6) reference configurations.

Table S2. Calculated singlet-triplet energy differences ($\Delta E = E(S_i) - E(T_j)$) in eV for IC at the TDDFT/cc-pVTZ level of theory in the gas phase and in media of variable dielectric constant ϵ (PCM solvation model)²⁵; we use the parameters for water and only change the dielectric constant to modify the properties of the medium). The calculations are done on B3LYP/6-31G(d) optimized geometries. The TDDFT approach is used to optimize the geometry of the excited states.^a

	Gas phase	Gas phase	$\epsilon = 2$	$\epsilon = 5$	$\epsilon = 10$	$\epsilon = 50$	$\epsilon = 78.35$
	S_0 optimized geometry	S_1 optimized geometry ^c					
$\Delta E (S_1-T_1)$	0.47	0.32	0.43	0.52	0.56	0.60	0.60
$\Delta E (S_1-T_2)$	0.54	0.48	0.50	0.55	0.46	0.43	0.43
$\Delta E (S_1-T_3)$	-0.95 ^b	-1.28 ^b	-1.20 ^b	-1.15 ^b	-1.10	-1.06	-1.05
	S_0 optimized geometry	S_2 optimized geometry ^c					
$\Delta E (S_2-T_1)$	1.43	1.19	1.24	-1.35	1.40	1.44	1.44
$\Delta E (S_2-T_2)$	1.51	1.13	1.00	-0.95	0.93	0.91	0.90
$\Delta E (S_2-T_3)$	0.01	-0.40	-0.47	0.44	-0.43	-0.41	-0.41

- a) The electronic states are characterized by the following electronic excitations with respect to the ($\dots 20\sigma 21\sigma^2 4\pi^2$) electronic configuration of the ground state S_0 : $21\sigma \rightarrow 5\pi$ for S_1 ; $4\pi \rightarrow 5\pi$ for S_2 ; $4\pi \rightarrow 5\pi$ for T_1 ; $21\sigma \rightarrow 5\pi$ for T_2 ; and $3\pi \rightarrow 5\pi$ for T_3 . See the figure below for the electronic characterization of the orbitals involved.
- b) For the gas phase and for $\epsilon = 2$ and $\epsilon = 5$, T_3 is characterized by the $20\sigma \rightarrow 5\pi$ excitation relative to the ground state electronic configuration.
- c) The cartesian coordinates of the optimized geometries are collected in Table S3 and some selected distances are collected in Table S4. The TDDFT optimized geometry of S_2 in gas phase has an imaginary frequency, which could not be eliminated by further minimization.



Contour plots of the most significant orbitals according to B3LYP/cc-pVTZ//B3LYP/6-31G(d) computations for the ground state of IC

Table S3. Cartesian coordinates (in Angstrom) for all IC optimized structures used in this work. The calculations include the optimized geometries for S_0 and T_1 in gas phase and bulk water, and the optimized geometries of the excited singlets S_1 and S_2 in gas phase, bulk water and other dielectric media. Calculations have been done at the B3LYP/6-31G(d) level, using the time-dependent density-functional theory approach (TDDFT) in the case of the excited singlets S_1 and S_2 . The optimizations in dielectric media have been done using the PCM model.²⁵

Gas phase

S_0 . Gas phase			
C	-.001681	.373735	.000000
C	-1.752185	-.856157	.000000
C	-.672570	-1.724789	.000000
N	.433028	-.925631	.000000
N	-1.328876	.439785	.000000
H	1.408029	-1.195310	.000000
H	-.608690	-2.802786	.000000
H	-2.803681	-1.109917	.000000
C	.935035	1.490479	.000000
H	.459917	2.489418	.000000
O	2.146950	1.334124	.000000
S_1 . Gas phase			
C	.033558	.374771	.000000
C	-1.743212	-.842614	.000000
C	-.682982	-1.734299	.000000
N	.451207	-.955431	.000000
N	-1.323010	.444864	.000000
H	1.404404	-1.284820	.000000
H	-.640248	-2.812789	.000000
H	-2.797883	-1.086760	.000000
C	.879980	1.471814	.000000
H	.442187	2.476921	.000000
O	2.191273	1.461294	.000000
S_2 . Gas phase			
C	-.109962	.444086	.000000
C	-1.780983	-.901098	.000000
C	-.637101	-1.731639	.000000
N	.410400	-.880814	.000000
N	-1.423587	.454076	.000000
H	1.418801	-1.014279	.000000
H	-.540498	-2.806990	.000000
H	-2.818030	-1.209954	.000000
C	.936568	1.514199	.000000
H	.638647	2.566741	.000000
O	2.121021	1.078622	.000000
T_1 . Gas phase			
C	-0.000000	0.423331	.000000
C	-1.774885	-0.811343	.000000
C	-0.659958	-1.718118	.000000
N	0.448142	-0.916752	.000000
N	-1.411072	0.451653	.000000
H	1.429126	-1.153583	.000000
H	-0.618436	-2.796922	.000000
H	-2.819173	-1.105698	.000000
C	0.912733	1.476082	.000000
H	0.532396	2.503803	.000000
O	2.168658	1.198547	.000000

Bulk water

S₀. (PCM with $\epsilon = 78.35$)

C	-0.000000	0.354463	.000000
C	-1.754081	-0.877903	.000000
C	-0.669276	-1.743919	.000000
N	0.431458	-0.945027	.000000
N	-1.332449	0.417499	.000000
H	1.401324	-1.235927	.000000
H	-0.601641	-2.821306	.000000
H	-2.803885	-1.138742	.000000
C	0.906510	1.490474	.000000
H	0.397722	2.472490	.000000
O	2.126812	1.384685	.000000

S₁. (PCM with $\epsilon = 78.35$)

C	.027542	.376593	.000000
C	-1.747595	-.849272	.000000
C	-.681829	-1.732102	.000000
N	.445278	-.947911	.000000
N	-1.329925	.445584	.000000
H	1.400120	-1.278008	.000000
H	-.630264	-2.809900	.000000
H	-2.800608	-1.100717	.000000
C	.879377	1.476931	.000000
H	.460553	2.489612	.000000
O	2.192628	1.442141	.000000

S₂. (PCM with $\epsilon = 78.35$)

C	-.060610	.421743	.000000
C	-1.775567	-.869249	.000000
C	-.642094	-1.730499	.000000
N	.426632	-.906522	.000000
N	-1.400156	.451248	.000000
H	1.416538	-1.122722	.000000
H	-.569203	-2.807971	.000000
H	-2.814374	-1.172510	.000000
C	.927911	1.512437	.000000
H	.552956	2.544360	.000000
O	2.153243	1.192635	.000000

T₁. (PCM with $\epsilon = 78.35$)

C	-0.000000	0.404786	.000000
C	-1.759146	-0.856031	.000000
C	-0.629314	-1.740534	.000000
N	0.463957	-0.921277	.000000
N	-1.408489	0.416895	.000000
H	1.441514	-1.174336	.000000
H	-0.567656	-2.817953	.000000
H	-2.796712	-1.169883	.000000
C	0.875818	1.497093	.000000
H	0.438878	2.503072	.000000
O	2.146444	1.294736	.000000

Other dielectric media

S₁. (PCM with $\epsilon = 2$)

C	.029456	.376550	.000000
C	-1.744939	-.845670	.000000
C	-.681972	-1.733188	.000000
N	.448865	-.951124	.000000
N	-1.327214	.445001	.000000
H	1.403213	-1.279137	.000000

H	-.635209	-2.811419	.000000
H	-2.798808	-1.093233	.000000
C	.878778	1.474110	.000000
H	.451412	2.483089	.000000
O	2.191695	1.447972	.000000
S ₁ . (PCM with e = 5)			
C	.027542	.376608	.000000
C	-1.746412	-.848005	.000000
C	-.681509	-1.732228	.000000
N	.446744	-.948504	.000000
N	-1.329402	.445737	.000000
H	1.401412	-1.277633	.000000
H	-.631369	-2.810240	.000000
H	-2.799651	-1.097954	.000000
C	.878454	1.475841	.000000
H	.457636	2.487426	.000000
O	2.191834	1.441903	.000000
S ₁ . (PCM with e = 10)			
C	.027416	.376659	.000000
C	-1.746905	-.848592	.000000
C	-.681606	-1.732137	.000000
N	.446077	-.948168	.000000
N	-1.329750	.445775	.000000
H	1.400805	-1.277855	.000000
H	-.630792	-2.810050	.000000
H	-2.800000	-1.099362	.000000
C	.878786	1.476434	.000000
H	.459084	2.488575	.000000
O	2.192163	1.441672	.000000
S ₁ . (PCM with e = 50)			
C	.027542	.376593	.000000
C	-1.747595	-.849272	.000000
C	-.681829	-1.732102	.000000
N	.445278	-.947911	.000000
N	-1.329925	.445584	.000000
H	1.400120	-1.278008	.000000
H	-.630264	-2.809900	.000000
H	-2.800608	-1.100717	.000000
C	.879377	1.476931	.000000
H	.460553	2.489612	.000000
O	2.192628	1.442141	.000000
S ₂ . (PCM with e = 2)			
C	-.091487	.435331	.000000
C	-1.779149	-.887862	.000000
C	-.638712	-1.730986	.000000
N	.417163	-.890313	.000000
N	-1.415446	.452030	.000000
H	1.418446	-1.057039	.000000
H	-.550806	-2.807174	.000000
H	-2.816670	-1.195426	.000000
C	.932965	1.513874	.000000
H	.605095	2.559038	.000000
O	2.133878	1.121477	.000000
S ₂ . (PCM with e = 5)			
C	-.074217	.427616	.000000
C	-1.776843	-.876886	.000000
C	-.640629	-1.730797	.000000
N	.422766	-.899346	.000000
N	-1.407035	.451691	.000000
H	1.417513	-1.094949	.000000
H	-.560890	-2.807729	.000000
H	-2.815068	-1.182069	.000000
C	.930026	1.513257	.000000

H	.574962	2.551043	.000000
O	2.144690	1.161120	.000000
S ₂ . (PCM with e = 10)			
C	-.067096	.424642	.000000
C	-1.776108	-.872916	.000000
C	-.641369	-1.730674	.000000
N	.424860	-.903264	.000000
N	-1.403257	.451580	.000000
H	1.416967	-1.110179	.000000
H	-.565300	-2.807903	.000000
H	-2.814663	-1.176953	.000000
C	.928921	1.513095	.000000
H	.563116	2.547724	.000000
O	2.149205	1.177799	.000000
S ₂ . (PCM with e = 50)			
C	-.060610	.421743	.000000
C	-1.775567	-.869249	.000000
C	-.642094	-1.730499	.000000
N	.426632	-.906522	.000000
N	-1.400156	.451248	.000000
H	1.416538	-1.122722	.000000
H	-.569203	-2.807971	.000000
H	-2.814374	-1.172510	.000000
C	.927911	1.512437	.000000
H	.552956	2.544360	.000000
O	2.153243	1.192635	.000000

Table S4. Selected interatomic distances (in Angstrom) corresponding to the optimized geometries in Table S3. The atom numbering is defined in Figure 2 of the main text. Calculations have been done at the B3LYP/6-31G(d) level, using the time-dependent density-functional theory approach (TDDFT) in the case of the excited singlets S_1 and S_2 . The optimizations in dielectric media have been done using the PCM model.²⁵

State	Method	d(1-4)	d(3-4)	d(2-3)	d(2-5)	d(1-5)	d(1-9)	d(9-11)
Gas phase								
S_0	B3LYP, gas phase	1.370	1.364	1.386	1.363	1.329	1.458	1.222
S_1	TDDFT, gas phase	1.394	1.376	1.385	1.354	1.358	1.386	1.311
S_2	TDDFT, gas phase	1.423	1.350	1.414	1.402	1.314	1.497	1.262
T_1	B3LYP, gas phase	1.413	1.367	1.437	1.314	1.412	1.394	1.286
Bulk water								
S_0	B3LYP, PCM, $\epsilon = 78$	1.369	1.360	1.388	1.362	1.334	1.453	1.225
S_1	TDDFT, PCM, $\epsilon = 78$	1.389	1.373	1.384	1.360	1.359	1.392	1.314
S_2	TDDFT, PCM, $\epsilon = 78$	1.415	1.349	1.424	1.373	1.340	1.262	
T_1	B3LYP, PCM, $\epsilon = 78$	1.405	1.366	1.435	1.320	1.409	1.400	1.287
Other dielectric media								
S_1	TDDFT, PCM, $\epsilon = 2$	1.392	1.375	1.384	1.357	1.358	1.388	1.313
S_1	TDDFT, PCM, $\epsilon = 5$	1.390	1.374	1.384	1.359	1.359	1.390	1.314
S_1	TDDFT, PCM, $\epsilon = 10$	1.389	1.373	1.384	1.360	1.359	1.391	1.314
S_1	TDDFT, PCM, $\epsilon = 50$	1.389	1.373	1.384	1.361	1.359	1.392	1.314
S_2	TDDFT, PCM, $\epsilon = 2$	1.420	1.350	1.418	1.388	1.324	1.488	1.263
S_2	TDDFT, PCM, $\epsilon = 5$	1.417	1.350	1.421	1.379	1.333	1.478	1.265
S_2	TDDFT, PCM, $\epsilon = 10$	1.416	1.350	1.422	1.376	1.336	1.475	1.266
S_2	TDDFT, PCM, $\epsilon = 50$	1.415	1.349	1.424	1.373	1.340	1.472	1.266

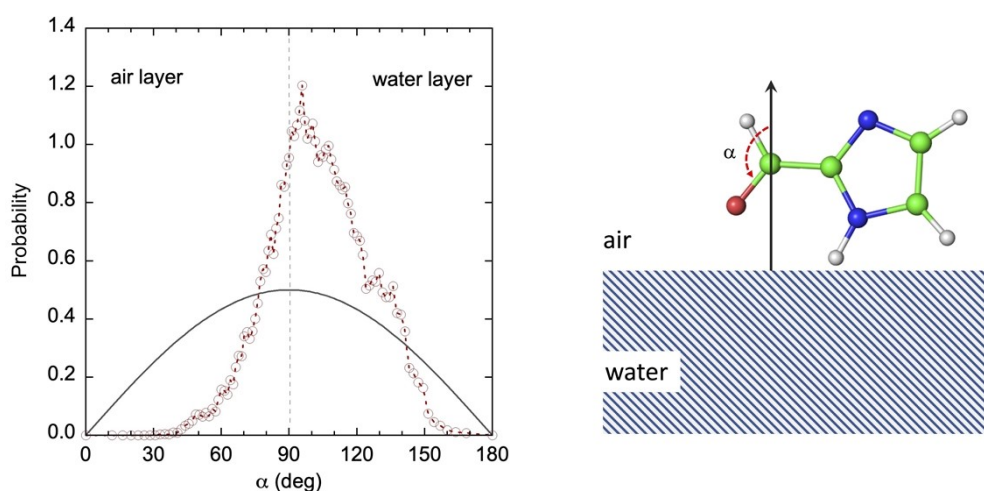


Figure S1. Angular distribution of IC at the air–water interface from the QM/MM molecular dynamics simulation. The distribution corresponds to the angle α formed by a vector perpendicular to the water surface and pointing towards the air layer with the C=O bond vector, as indicated in the right part of the Figure. The black line corresponds to the uniform distribution $\frac{1}{2} \sin \theta$.

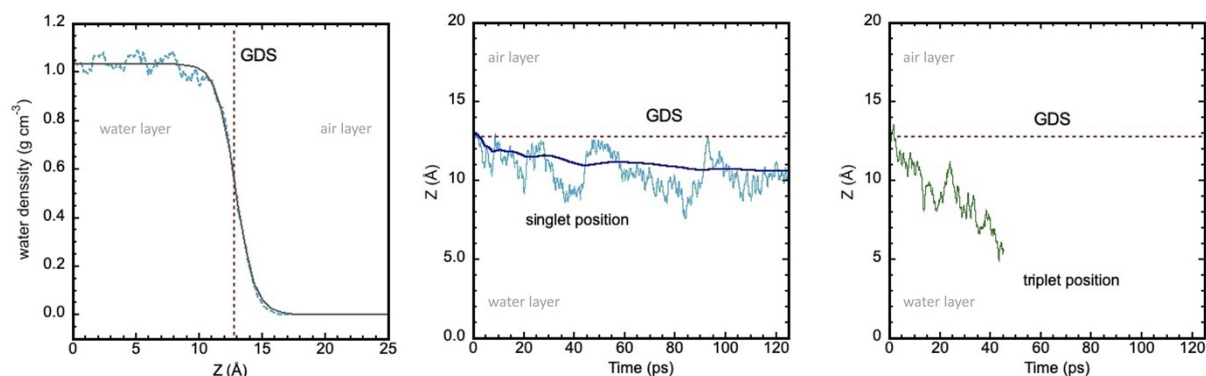


Figure S2. Position of IC with respect to the formal interface along the QM/MM MD simulations of the singlet ground state S_0 and the lowest triplet state T_1 at the air-water interface. $Z=0$ corresponds to the centre of the simulation box.

Left: water density profile from the IC(S_0) simulation (dashed blue line) and fitted profile (black plain line) allowing to define the formal interface at $Z=+12.9$ Å (Gibbs dividing surface, GDS, red dashed line)). A similar profile is obtained for negative values of Z . The results for the IC(T_1) simulation are comparable.

Middle: instantaneous position of the IC centre of mass (light blue line) and average value (dark blue line) in the IC(S_0) simulation.

Right: instantaneous position of the IC centre of mass in the IC(T_1) simulation (green line).

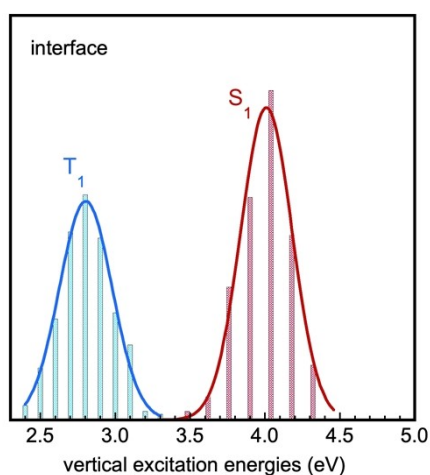


Figure S3. The figure illustrates the fit by Gaussian functions of the calculated vertical excitation energies histograms (Figure 6 of the paper) in the case of S_1 and T_1 at the air-water interface. The bars in the figure correspond to the values of the bins using intervals of 0.14 eV. The plain lines correspond to the fitted Gaussians.

References

1. M. J. Field, P. A. Bash and M. Karplus, *J. Comput. Chem.*, 1990, **11**, 700-733.
2. A. Warshel and M. Levitt, *J. Mol. Biol.*, 1976, **103**, 227-249.
3. I. Tuñón, M. T. C. Martins-Costa, C. Millot and M. F. Ruiz-López, *J. Mol. Mod.*, 1995, **1**, 196-201.
4. I. Tuñón, M. T. C. Martins-Costa, C. Millot and M. F. Ruiz-Lopez, *Chem. Phys. Lett.*, 1995, **241**, 450-456.
5. I. Tuñón, M. T. C. Martins-Costa, C. Millot and M. F. Ruiz-López, *J. Chem. Phys.*, 1997, **106**, 3633-3642.
6. A. D. Becke, *J. Chem. Phys.*, 1993, **98**, 5648-5652.
7. W. J. Hehre, R. Ditchfield and J. A. Pople, *J. Chem. Phys.*, 1972, **56**, 2257-2261.
8. R. Krishnan, J. S. Binkley, R. Seeger and J. A. Pople, *J. Chem. Phys.*, 1980, **72**, 650-654.
9. W. L. Jorgensen, J. Chandrashekar, J. D. Madura, W. R. Impey and M. L. Klein, *J. Chem. Phys.*, 1983, **79**, 926-935.
10. L. X. Dang and B. M. Pettitt, *J. Phys. Chem.*, 1987, **91**, 3349-3354.
11. R. S. Taylor, L. X. Dang and B. C. Garrett, *J. Phys. Chem.*, 1996, **100**, 11720-11725.
12. W. G. Hoover, *Phys. Rev. A* 1985, **31**, 1695-1697.
13. S. Nosé, *The Journal of Chemical Physics* 1984, **81**, 511-519.
14. A Gaussian 09 / Tinker 4.2 interface for hybrid QM/MM applications., M. T. C. Martins-Costa, University of Lorraine - CNRS 2014
15. Gaussian 09, M. J. Frisch, G. W. Trucks, H. B. Schlegel, G. E. Scuseria, M. A. Robb, J. R. Cheeseman, G. Scalmani, V. Barone, B. Mennucci, G. A. Petersson, H. Nakatsuji, M. Caricato, X. Li, H. P. Hratchian, A. F. Izmaylov, J. Bloino, G. Zheng, J. L. Sonnenberg, M. Hada, M. Ehara, K. Toyota, R. Fukuda, J. Hasegawa, M. Ishida, T. Nakajima, Y. Honda, O. Kitao, H. Nakai, T. Vreven, J. A. Montgomery Jr., J. E. Peralta, F. Ogliaro, M. J. Bearpark, J. Heyd, E. N. Brothers, K. N. Kudin, V. N. Staroverov, R. Kobayashi, J. Normand, K. Raghavachari, A. P. Rendell, J. C. Burant, S. S. Iyengar, J. Tomasi, M. Cossi, N. Rega, N. J. Millam, M. Klene, J. E. Knox, J. B. Cross, V. Bakken, C. Adamo, J. Jaramillo, R. Gomperts, R. E. Stratmann, O. Yazyev, A. J. Austin, R. Cammi, C. Pomelli, J. W. Ochterski, R. L. Martin, K. Morokuma, V. G. Zakrzewski, G. A. Voth, P. Salvador, J. J. Dannenberg, S. Dapprich, A. D. Daniels, Ö. Farkas, J. B. Foresman, J. V. Ortiz, J. Cioslowski and D. J. Fox, Gaussian, Inc. 2009
16. TINKER: Software Tools for Molecular Design 4.2, J. W. Ponder, Washington University School of Medicine: Saint Louis, MO. 2004
17. T. H. J. Dunning, *J. Chem. Phys.*, 1989, **90**, 1007-1023.
18. F. Neese, *WIREs Comput. Mol. Sci.*, 2012, **2**, 73-78.
19. B. Valeur and M. N. Berberan-Santos, *Molecular fluorescence: principles and applications*, John Wiley & Sons, 2012.
20. A. Serr and N. O'Boyle, ed. Zenodo, 2017, p. <https://doi.org/10.5281/zenodo.820871>.
21. J. M. Anglada, M. T. C. Martins-Costa, M. F. Ruiz-Lopez and J. S. Francisco, *Proc. Natl. Acad. Sci. USA*, 2014, **111**, 11618-11623.
22. M. T. C. Martins-Costa, J. M. Anglada, J. S. Francisco and M. F. Ruiz-López, *Phys. Chem. Chem. Phys.*, 2017, **19**, 31621-31627.
23. M. T. C. Martins-Costa, J. M. Anglada, J. S. Francisco and M. F. Ruiz-Lopez, *Chem. Eur. J.*, 2019, **25**, 13899-13904.
24. M. T. C. Martins-Costa, J. M. Anglada, J. S. Francisco and M. F. Ruiz-López, *J. Am. Chem. Soc.*, 2018, **140**, 12341-12344.
25. J. Tomasi, B. Mennucci and E. Cancès, *J. Mol. Struct.: THEOCHEM*, 1999, **464**, 211-226.